Life Sciences 217 (2019) 176–184

Contents lists available at ScienceDirect

Life Sciences

journal homepage: www.elsevier.com/locate/lifescie

A comparative study of the efficiency of HCV NS3/4A protease drugs against different HCV genotypes using in silico approaches

Ahmed A. Ezat*, Wael M. Elshemey

Biophysics Department, Faculty of Science, Cairo University, 12613 Giza, Egypt

ARTICLE INFO

Keywords:
HCV
NS3/4A protease
Molecular docking
Homology modeling

ABSTRACT

Aims: To investigate the efficacy of Direct Acting Antivirals (DAAs) in the treatment of different Hepatitis C Virus (HCV) genotypes.

Main methods: Homology modeling is used to predict the 3D structures of different genotypes while molecular docking is employed to predict genotype – drug interactions (Binding Mode) and binding free energy (Docking Score).

Key findings: Simeprevir (TMC435) and to a lesser degree MK6325 are the best drugs among the studied drugs. The predicted affinity of drugs against genotype 1a is always better than other genotypes. P2–P4 macrocyclic drugs show better performance against genotypes 2, 3 and 5. Macrocyclic drugs are better than linear drugs.

Significance: HCV is one of the major health problems worldwide. Until the discovery of DAAs, HCV treatment faced many failures. DAAs target key functional machines of the virus life cycle and shut it down. NS3/4A protease is an important target and several drugs have been designed to inhibit its functions. There are several NS3/4A protease drugs approved by Food and Drug Administration (FDA). Unfortunately, the virus exhibits resistance against these drugs. This study is significant in elucidating that no one drug is able to treat different genotypes with the same efficiency. Therefore, treatment should be prescribed based on the HCV genotype.

1. Introduction

Hepatitis C Virus (HCV) is the causative agent of liver hepatitis C. If it remains untreated, it may develop to liver cirrhosis, fibrosis and hepatocellular carcinoma. Around 180 million people are infected with HCV worldwide [1,2]. HCV replication is very fast and error prone due to the low fidelity of NS5B RNA polymerase. As a consequence, the virus is present as a large population of viral variants in patients [3]. There are seven genotypes and several subtypes of HCV that are identified up till now [1]. They differ in their sequences, geographic distribution and response to available treatments [1,4]. Genotype 1 is prevalent in Europe and North America [1]. It is the most widely studied genotype and most of the designed drugs are tailored based on it. For long time, the standard of care was Pegylated-interferon α and ribavirin, but it wasn't so effective against genotype 1 and had several side effects [3,5,6]. So, there was an urgent medical need to discover novel HCV treatments. Direct Acting Antivirals (DAAs) are the best solutions to this problem [5,6]. They target key components of the virus life cycle and shut it down. NS3/4A protease, NS5A and NS5B proteins are the best targets for designed DAAs [3]. Food and Drug Administration (FDA) approved many drugs from 2011 up till now [5,6]. These drugs are mainly NS3/4A protease inhibitors such as boceprevir, telaprevir, simeprevir, grazoprevir, paritaprevir and recently glecaprevir. These drugs are now part of all-oral, interferon-free therapies and show high success rates [5,6].

NS3/4A is a bifunctional protein [3,7–9]. It contains N-terminal serine protease domain and C-terminal DExH/D helicase and NTPase functionalities. The serine protease domain belongs to the chymotrypsin superfamily [7–9]. It contains H57, D81 and S139 as the catalytic triad that catalyze the peptide hydrolysis at four downstream junctions of the large HCV polyprotein [3,7]. It also attacks two important signaling proteins, MAVS and TRIF, which activate the immune system against the viral infection [10–12]. The inhibition of NS3/4A protease has two effects: it prevents the maturation of viral proteins and restores the host immune response [7–9].

Unfortunately, the approved drugs suffer from failure in many cases [5,6]. Several mutations occur in the binding site of NS3/4A protease, which affect drug binding and cause drug resistance [13]. It is a big challenge and needs more efforts to be done. This is the reason why research is still concerned with the design of new drugs and the search for new strategies to fight against drug resistance [14–18]. Also, there are genotypes that are still difficult to treat, such as genotypes 2 and 3

* Corresponding author.
E-mail address: ezat@sci.cu.edu.eg (A.A. Ezat).

https://doi.org/10.1016/j.lfs.2018.12.004
Received 19 September 2018; Received in revised form 21 November 2018; Accepted 3 December 2018
Available online 04 December 2018
0024-3205/

[2,6,13,19]. They have natural polymorphisms (variants) that cause resistance to several drugs [13,19]. Several studies report that the dynamics of different genotypes are not conserved [19–21]. This explains their different enzymatic activities, drug affinities and response to treatment. The physicochemical and geometrical characteristics of binding sites are not conserved as well [19–21].

Molecular modeling techniques are well established tools for the study of the dynamics, energetics and interactions of biomolecules, especially proteins [22–26]. They are widely used to study protein – ligand interactions and to predict the binding mode of a drug inside the binding site of a protein [8,9]. Molecular docking is one of these techniques that is able to predict the binding mode of drugs with protein (i.e. protein – drug complex conformation) and score of complex (i.e. binding free energy of complex) [27–29].

In this study, the efficacy of several NS3/4A protease inhibitors (approved or in clinical trials) against several HCV genotypes are compared using molecular modeling approaches. The binding interactions of best drugs with HCV genotypes are discussed in order to explain the difference in drug affinities against different genotypes. In the era of personalized medicine, this will aid to prescribe the best drug to a patient according to his/her HCV genotype. It will help in the design of new potent drugs through taking the pitfalls of current drugs into account.

2. Materials and methods

2.1. Sequence analysis and protein homology modeling

The sequences of HCV NS3/4A protease of 18 different genotypes are retrieved from UniProt database [30]. Only the reviewed sequences are retrieved. The sequences ID's are listed in Table 1. The genotypes are 1a, 1b, 1c, 2a, 2b, 2c, 2k, 3a, 3b, 3k, 4a, 5a, 6a, 6b, 6d, 6g, 6h, and 6k. Multiple sequences alignment are performed using MUSCLE server [31] and it is rendered using Esprit [32] to show the conserved and variable regions and the secondary structure of the protein.

Models are built for each sequence where there is no available crystal structure. Only 1a (5VOJ) [17], 1b (4I31) [33] and 3a (5EQS) [19] have crystal structures and no model building is done for these sequences. Genotype 3a structure is a chimeric 3a/1a [19]. Modeling is done using SWISS MODEL server [34] (Automated Mode). The models are retrieved and submitted to GalaxyRefine [35] for further refinement. It rebuilds the side chains of model and then relaxes the structure by performing short molecular dynamics simulations. The accuracy of the produced model is superior to that of the initial model in terms of global (overall fold and packing) and local (side chain rotamers and local environment of residues) quality [35].

GalaxyRefine produces 5 models of the protein after molecular dynamics relaxation. All of the 5 models are validated using different servers (SAVES and MolProbity servers [36,37]) to pick the best model. These servers check the stereo-chemical quality of the protein model (bond lengths, angles, dihedrals and side chain conformations), the packing of atoms inside the hydrophobic core and the non-bonded interactions of atoms and how much it deviates from the distribution of high quality experimental structures. The cofactor 4A is added to the protein model using Swiss PDB viewer by aligning the model with 1b crystal structure (4I31) and merging the cofactor coordinates with the model. The cofactor is then mutated to the sequence of genotype. The whole model is further energy minimized to remove any steric clashes. The models are now ready for further computational studies.

The physicochemical and geometrical characteristics of the different genotypes' binding sites are predicted using DoGSiteScorer server [38].

2.2. Ligand modeling

The coordinates of solved ligand structures (Simeprevir “SIM”, Vaniprevir “VAN”, Grazoprevir “GRZ”, Asunaprevir “ASN” and Danoprevir “DAN”) are retrieved from RSCB protein data bank. The 3D coordinates of other ligands that don't have any crystal structure are generated by Openbabel [39] by converting their smiles strings (Paritaprevir “PAR”, Glecaprevir “GLE”, Voxilaprevir “VOX”, Sovaprevir “SOV” and Deldeprevir “DEL”) to 3D structures. The smiles strings are retrieved from CHEMBL bioactivity database [40]. Only three structures (MK2748, MK6325 and MK8831), where no crystal structures or smiles strings are available, are built using SCIGRESS 3.0 software. These compounds are sketched, geometry optimized (MM3 molecular mechanics force field and PM6 semi-empirical quantum mechanics) using SCIGRESS 3.0 software [24–26]. The coordinates of 13 ligands are now ready.

2.3. Molecular docking simulations

Docking simulations are performed using Autodock Vina software [41,42]. Both ligands and proteins are prepared for docking using Autodock tools [42]. The missing hydrogens and charges are added. The ligands are treated as flexible while the protein as rigid except some side chains of the active site which are flexible (H57, D81, K136, S139 and R155). The center of grid box is chosen between the catalytic triad and the box dimensions are chosen to cover all the flexible residues. The box dimensions are set to 26 with grid spacing of 1A°.

There are solved crystal structures of some ligands with genotype 1a

Table 1
The physicochemical characteristics of different genotypes' binding sites as predicted by DoGSiteScorer server. The sequence IDs are in parenthesis.

	Volume	Surface area	Depth	Pocket atoms	H bonds donors	H bonds acceptors	Hydrophobic interactions
1A (P26664)	304.5	559.5	12.83	82	12	14	35
1B (Q9WMX2)	315.5	447.8	11.58	72	9	18	24
1C (Q81754)	296.9	490.8	15.47	74	7	22	31
2A (P26660)	244.61	407.85	11.31	60	7	16	22
2B (Q9DHD6)	275.58	481.34	14.81	80	10	22	30
2C (Q68749)	245.57	423.78	11.56	62	7	16	18
2K (Q9QAX1)	292.48	520.34	15.33	85	12	24	27
3A (Q81495)	409.34	691.45	11.67	87	19	20	30
3B (Q81487)	392.06	641.48	15.47	93	15	24	34
3K (Q68801)	330.18	515.09	14.44	76	6	22	24
4A (O39929)	359.10	613.68	14.02	73	15	22	29
5A (O39928)	362.50	533.10	14.93	93	13	24	31
6A (Q5I2N3)	304.19	415.97	14.39	78	8	24	22
6B (O92529)	247.04	468.61	13.03	63	8	18	25
6D (O92530)	326.78	443.36	14.76	70	5	20	24
6G (Q68798)	267.58	413.53	14.77	76	8	22	25
6H (O92532)	407.17	592.91	15.17	84	14	24	29
6K (O92531)	331.20	468.42	14.82	79	7	20	27

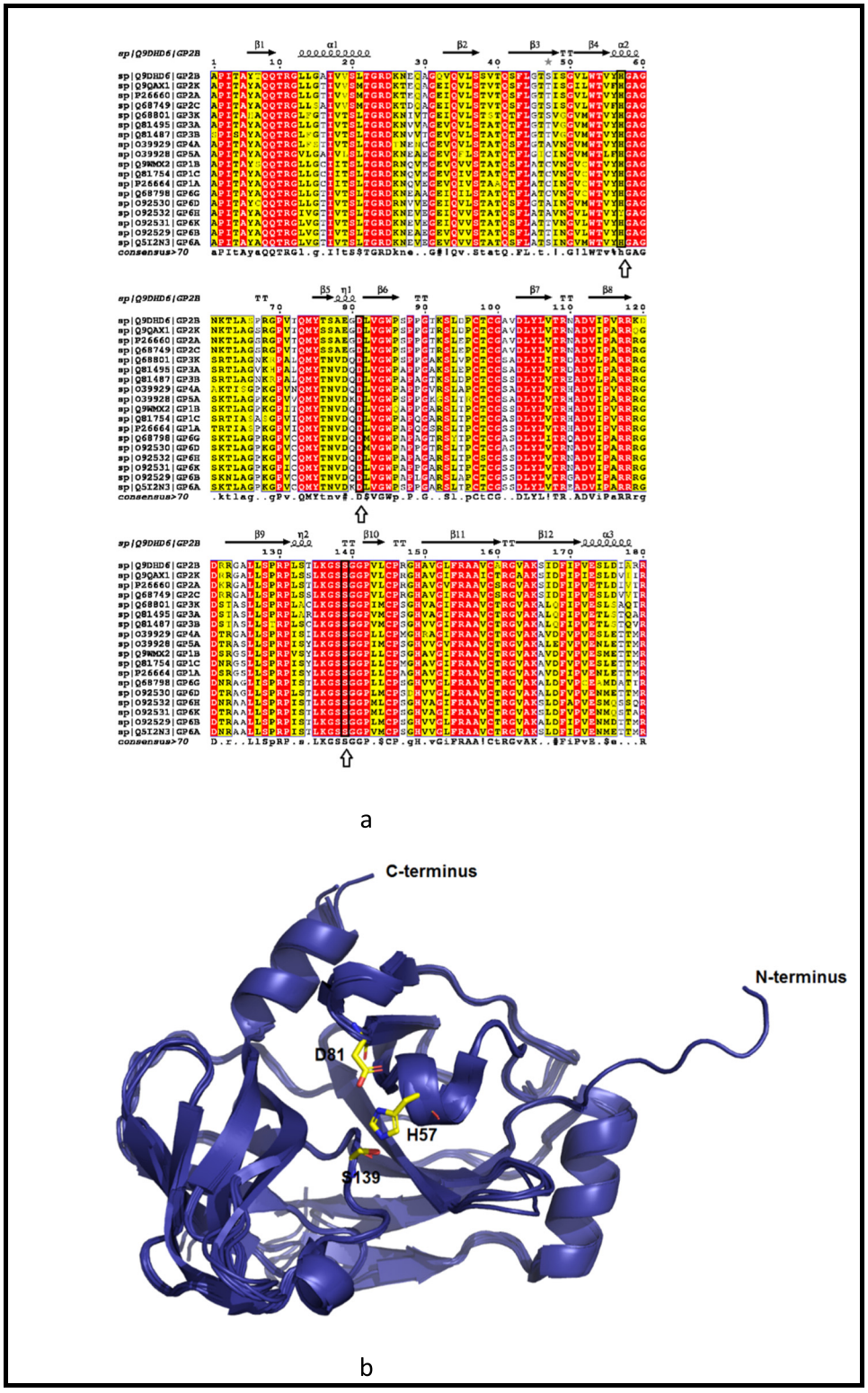

Fig. 1. Shows [A] multiple sequence alignment. Red color represents conserved residues, yellow represents less conserved while white color represents variable residues. The arrows represent active site residues H/Y57, D81 and S139 [B] Structural alignment of genotypes 1–6. The active site residues H57, D81 and S139 are shown in yellow sticks. Only subtypes "A" are presented for clarity. (For interpretation of the references to color in this figure legend, the reader is referred to the web version of this article.)

(Vaniprevir, Danoprevir, Asunaprevir and Grazoprevir), 1b (Simeprevir and Danoprevir) and 3a (Vaniprevir, Danoprevir and Asunaprevir). These structures are just scored using score - only option of Autodock vina [41]. The PDB codes of these structures are listed in table S1 (Supplementary info).

Protein – Ligand Interaction Profiler (PLIP) [43] is used to get the different interactions, especially hydrogen bonds and hydrophobic interactions between the protein and ligand and to analyze the binding mode of the best drugs with different genotypes.

Validation of the docking protocol is carried out through re-docking

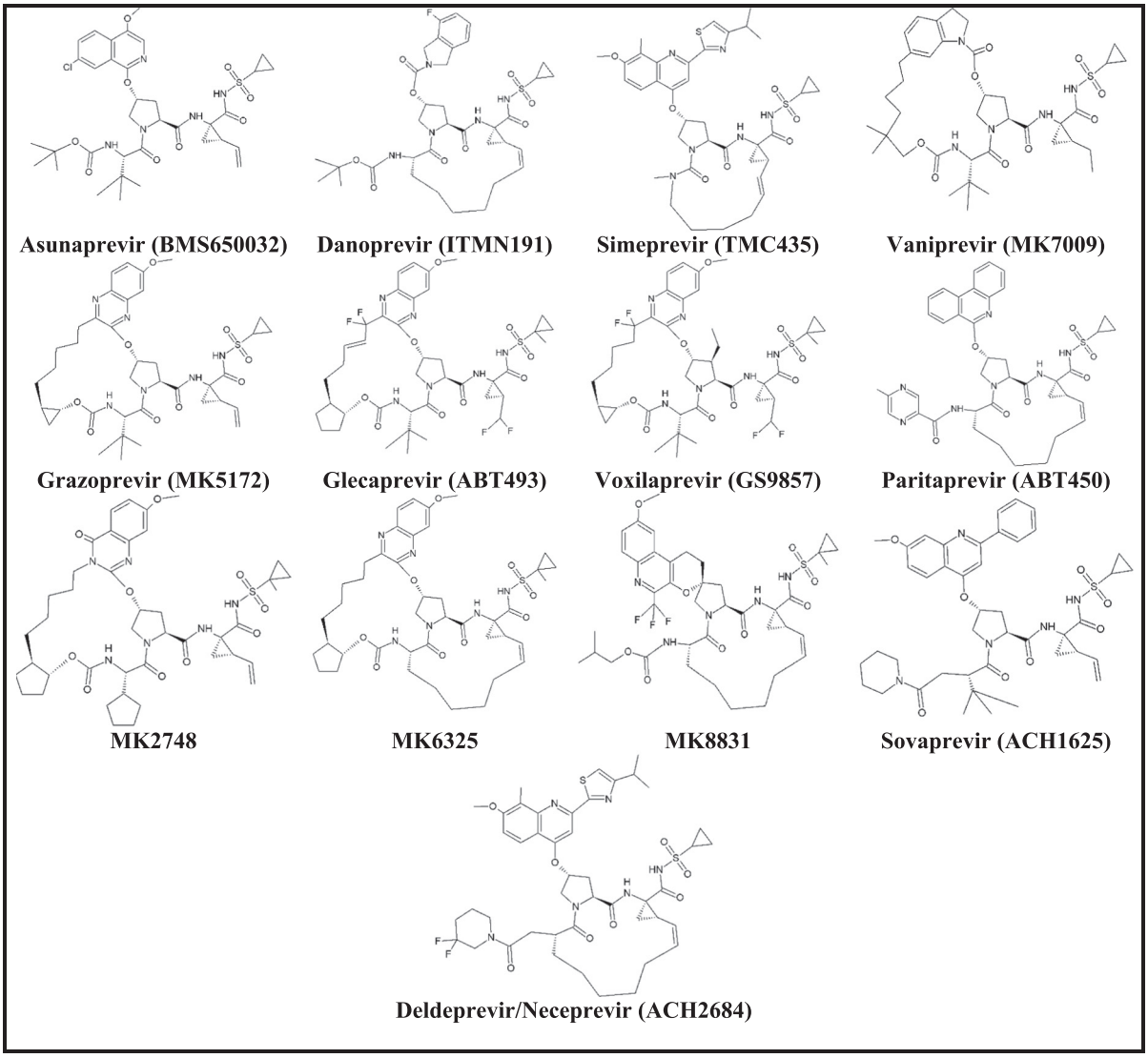

Fig. 2. Presents chemical structures of studied drugs.

of ligands into their holo crystal structures to see if the protocol can reproduce the ligand binding mode. Three crystal structures (5VOJ, 4I31 and 5EQS) are used for the re-docking study. These structures represent the structures of 1a, 1b and 3a that are further used for docking. The ligands are taken from the crystal structures and re-docked back using the same protocol. RMSD between experimental and re-docked structures is calculated to see the difference between them and validate the docking protocol.

2.4. Statistical analysis

The simulations are repeated 3 times with random seeds to get good statistical results. The data are presented as Mean ± S.D. Statistical significance is set to 0.05 and the mean values are compared through Duncan multiple range test using SPSS 19.0 software package.

3. Results and discussion

3.1. Sequence analysis

The sequence alignment is presented in Fig. 1a. Different genotypes show higher similarity, especially in the binding site region. The conserved residues are colored in red while the less conserved residues are colored in yellow. White color represents variable residues at a certain position. The consensus sequence, with similarity more than 70%, is shown as well. The catalytic and oxyanion hole residues are conserved across all genotypes except for genotype 6 h, where the catalytic H57 is replaced by Y57. Several genotypes contain resistance associated variants [13,19]. Genotypes 2a, 2b, 2c and 2k have different amino acids in E1 – F1 loop (T76S, N77S, V78A, D79E and Q80G). Genotypes 3a, 3b and 3k have natural polymorphisms associated with resistance (R123T and D168Q) [13,19]. Genotype 5a contain Q80K and D168E [13,44,45], which are known as resistant variants while genotype 6a contain Q80K only. So, different genotypes are expected to interact differently to drugs and show different responses [6,13,19].

3.2. Homology modeling and model validation

One needs the structure of a protein to be able to study its interaction with different drugs. Only, the 3D structures of genotypes 1a, 1b and 3a are available. So, homology modeling techniques are used to build the models of different genotypes. SWISS MODEL server is used to do the homology modeling. It utilizes the protein sequence to provide a 3D model of the protein. The quality of model depends on the target – template alignment, quality and resolution of template 3D structure and the similarity between target and template [34]. As a rule of thumb, the

Table 2
The docking scores of different drugs versus different genotypes. Data are presented as Mean ± S.D. The best drugs for each genotype are presented in bold numbers. The different letters (a, b, c …) represent significant difference between the means.

	1A	1B	1C	2A	2B	2C
SIM	**−13.0 ± 0.0^{a}**	**−12.1 ± 0.0^{a}**	−9.4 ± 0.1^{b,c,d}	−9.5 ± 0.0^{b}	**−10.5 ± 0.1^{a}**	−9.3 ± 0.0^{b,c}
MK6325	−11.9 ± 0.0^{b}	−11.3 ± 0.1^{b,c}	**−10.5 ± 0.0^{a}**	**−9.7 ± 0.0^{a,b}**	−9.1 ± 0.0^{c,d}	**−9.7 ± 0.0^{a,b}**
DAN	−11.7 ± 0.0^{b}	−10.4 ± 0.0^{e}	−9.8 ± 0.2^{b,c}	−8.8 ± 0.1^{c}	−9.6 ± 0.0^{b}	−9.0 ± 0.0^{c,d}
VAN	−11.2 ± 0.0^{c}	**−12.2 ± 0.1^{a}**	**−10.0 ± 0.8^{a,b}**	**−9.9 ± 0.0^{a}**	−9.6 ± 0.1^{b}	−9.6 ± 0.3^{b}
PAR	−10.7 ± 0.0^{d}	−10.9 ± 0.0^{c,d}	−9.5 ± 0.0^{b,c}	**−9.9 ± 0.0^{a}**	−9.4 ± 0.5^{b,c}	**−10.1 ± 0.5^{a}**
GRZ	−10.5 ± 0.0^{d,e}	−11.5 ± 0.0^{b}	−9.7 ± 0.1^{b,c}	**−9.8 ± 0.2^{a,b}**	−9.0 ± 0.0^{d}	−9.5 ± 0.2^{b}
MK2748	−10.4 ± 0.0^{d,e}	−10.8 ± 0.0^{d}	−9.6 ± 0.2^{b,c}	−8.9 ± 0.0^{c}	**−10.6 ± 0.1^{a}**	**−10.1 ± 0.1^{a}**
GLE	−10.3 ± 0.4^{e}	−11.6 ± 0.1^{b}	−9.3 ± 0.2^{c,d}	−8.7 ± 0.0^{c,d}	−9.7 ± 0.2^{b}	−8.6 ± 0.3^{d,e}
VOX	−9.8 ± 0.0^{f}	−9.7 ± 0.1^{f}	−7.8 ± 0.1^{e}	−7.6 ± 0.4^{f}	−9.3 ± 0.0^{b,c,d}	−8.3 ± 0.2^{e}
DEL	−9.8 ± 0.2^{f}	−8.7 ± 0.0^{g}	−8.9 ± 0.0^{d}	−8.3 ± 0.3^{e}	−9.1 ± 0.1^{c,d}	−8.8 ± 0.3^{d,e}
SOV	−9.5 ± 0.0^{f}	−8.5 ± 0.6^{g}	−8.3 ± 0.2^{e}	−7.2 ± 0.1^{g}	−8.2 ± 0.2^{e}	−7.3 ± 0.2^{f}
ASN	−9.0 ± 0.0^{g}	−9.4 ± 0.0^{f}	−8.0 ± 0.1^{e}	−8.4 ± 0.0^{d,e}	−7.8 ± 0.2^{f}	−8.2 ± 0.1^{e}
MK8831	−8.6 ± 0.1^{h}	−8.7 ± 0.0^{g}	−8.2 ± 0.1^{e}	−8.2 ± 0.0^{e}	−8.1 ± 0.1^{e,f}	−8.2 ± 0.1^{e}

	2K	3A	3B	3K	4A	5A
SIM	**−9.9 ± 0.1^{a}**	**−11.5 ± 0.1^{a,b}**	−9.7 ± 0.1^{b,c}	−9.5 ± 0.3^{b}	−9.7 ± 0.1^{d,e}	−8.5 ± 0.1^{d}
MK6325	**−10.0 ± 0.0^{a}**	−11.1 ± 0.1^{c}	−9.9 ± 0.0^{b}	−9.1 ± 0.1^{b,c,d}	**−10.6 ± 0.0^{a}**	**−9.6 ± 0.1^{a}**
DAN	−9.1 ± 0.0^{c,d}	−10.9 ± 0.0^{c}	−9.4 ± 0.0^{d}	−9.4 ± 0.0^{b,c}	−9.6 ± 0.1^{d,e}	−9.1 ± 0.3^{b,c}
VAN	−8.6 ± 0.1^{d,e}	**−11.7 ± 0.0^{a}**	−9.0 ± 0.1^{e}	−8.7 ± 0.0^{d,e}	−9.9 ± 0.2^{c,d}	**−9.5 ± 0.2^{a}**
PAR	**−9.5 ± 0.5^{a,b,c}**	−10.9 ± 0.1^{c}	**−10.7 ± 0.0^{a}**	−9.2 ± 0.1^{b,c}	**−10.5 ± 0.3^{a,b}**	−9 ± 0.0^{c}
GRZ	−9.1 ± 0.0^{c,d}	**−11.8 ± 0.0^{a}**	−9.5 ± 0.1^{c,d}	−8.9 ± 0.4^{c,d}	−9.7 ± 0.2^{d,e}	**−9.8 ± 0.0^{a}**
MK2748	**−9.8 ± 0.7^{a,b}**	−10.6 ± 0.2^{d}	**−10.5 ± 0.2^{a}**	**−10.0 ± 0.3^{a}**	−10.2 ± 0.3^{b,c}	**−9.7 ± 0.1^{a}**
GLE	−9.2 ± 0.3^{b,c,d}	−11.3 ± 0.^{b,c}	−9.5 ± 0.0^{c,d}	−9.3 ± 0.1^{b,c}	−9.4 ± 0.3^{e}	**−9.4 ± 0.3^{a,b}**
VOX	−7.8 ± 0.1^{f,g}	−9.5 ± 0.4^{e}	−8.6 ± 0.0^{f}	−8.1 ± 0.1^{g}	−8.9 ± 0.1^{f}	−8.1 ± 0.0^{e}
DEL	−8.1 ± 0.0^{e,f}	−8.5 ± 0.3^{g}	−8.4 ± 0.1^{f,g}	−8.5 ± 0.1^{e,f}	−8.6 ± 0.16^{f,g}	−9.0 ± 0.0^{b,c}
SOV	−7.2 ± 0.1^{g}	−8.3 ± 0.0^{g}	−7.5 ± 0.1^{i}	−7.6 ± 0.1^{h}	−8.3 ± 0.1^{g}	−7.3 ± 0.3^{f}
ASN	−7.6 ± 0.2^{f,g}	−9.1 ± 0.0^{f}	−8.1 ± 0.1^{h}	−6.9 ± 0.1^{i}	−8.3 ± 0.1^{g}	−7.9 ± 0.1^{e}
MK8831	−8.1 ± 0.2^{e,f}	−8.3 ± 0.0^{g}	−8.3 ± 0.1^{g,h}	−8.2 ± 0.1^{f,g}	−8.9 ± 0.18^{f}	−7.9 ± 0.2^{e}

	6A	6B	6D	6G	6H	6K
SIM	−8.8 ± 0.2^{c}	**−10.7 ± 0.1^{a}**	**−11.0 ± 0.0^{a}**	−9.5 ± 0.1^{c,d}	−9.5 ± 0.2^{b}	**−10.5 ± 0.1^{a}**
MK6325	−9.5 ± 0.1^{b}	−9.5 ± 0.5^{c}	**−10.9 ± 0.1^{a}**	**−10.4 ± 0.1^{a}**	−9.6 ± 0.0^{b}	−9.5 ± 0.1^{c}
DAN	−8.7 ± 0.2^{c}	−9.4 ± 0.1^{c}	**−10.5 ± 0.0^{a,b,c}**	−8.3 ± 0.3^{f}	−9.4 ± 0.0^{b,c}	−9.2 ± 0.0^{c}
VAN	**−9.7 ± 0.1^{a,b}**	−9.8 ± 0.0^{b,c}	**−11.0 ± 0.0^{a}**	**−10.2 ± 0.0^{a,b}**	−9.4 ± 0.0^{b,c}	**−10.3 ± 0.1^{a}**
PAR	−8.9 ± 0.5^{c}	−9.4 ± 0.1^{c}	**−10.8 ± 0.2^{a,b}**	−9.1 ± 0.2^{d,e}	−9.5 ± 0.4^{b}	−9.4 ± 0.2^{b,c}
GRZ	−9.4 ± 0.1^{b}	−9.4 ± 0.3^{c}	−10.1 ± 0.0^{b,c,d}	−9.7 ± 0.0^{b,c}	**−10.1 ± 0.0^{a}**	−9.7 ± 0.0^{b}
MK2748	**−10.2 ± 0.2^{a}**	−10.0 ± 0.0^{b}	−9.6 ± 0.4^{d,e,f}	−9.0 ± 0.0^{d,e}	**−10.1 ± 0.1^{a}**	−9.7 ± 0.1^{b}
GLE	**−9.8 ± 0.1^{a,b}**	−9.4 ± 0.0^{c}	−9.8 ± 0.9^{c,d,e}	−9.0 ± 0.6^{d,e}	−9.3 ± 0.2^{b,c}	−9.5 ± 0.3^{b,c}
VOX	−7.7 ± 0.2^{d}	−7.8 ± 0.3^{e}	−8.1 ± 0.0^{h}	−8.0 ± 0.1^{f}	−8.8 ± 0.1^{d,e}	−7.8 ± 0.0^{e}
DEL	−7.8 ± 0.1^{d}	−8.5 ± 0.2^{d}	−9.4 ± 0.5^{d,e,f,g}	−8.9 ± 0.1^{d,e}	−9.2 ± 0.4^{b,c,d}	−8.1 ± 0.4^{e}
SOV	−7.5 ± 0.6^{d}	−8.0 ± 0.1^{e}	−8.7 ± 0.5^{g,h}	−8.6 ± 0.1^{e,f}	−8.9 ± 0.1^{c,d,e}	−7.9 ± 0.3^{e}
ASN	−7.8 ± 0.2^{d}	−7.9 ± 0.1^{e}	−8.8 ± 0.2^{f,g,h}	−7.4 ± 0.6^{g}	−7.9 ± 0.1^{f}	−8.7 ± 0.0^{d}
MK8831	−7.8 ± 0.0^{d}	−7.6 ± 0.1^{e}	−9.1 ± 0.1^{e,f,g}	−8.2 ± 0.0^{f}	−8.5 ± 0.0^{e}	−8.1 ± 0.2^{e}

higher the target – template sequence similarity, the higher the target model quality [34]. Although, the predicted models are good, further refinements are carried out using GalaxyRefine server [35]. It improves the quality of a protein model through conducting short molecular dynamics simulations. Molecular dynamics simulations are widely used to refine and relax the predicted 3D structures and to remove any undesired steric clashes [46]. GalaxyRefine gives 5 models which are better than the submitted model. SAVES and MolProbity servers [36,37] check the packing quality of amino acids, the non-bonded interactions and the stereo-chemistry of models. The best model for each genotype is selected based on these criteria. Superposition of genotypes 1–6 are presented in Fig. 1b. Only, the subtypes “a” are shown for clarity. DoGSiteScorer server gives a wealth of information about the binding sites' characteristics of different genotypes such as volume, surface area, hydrogen bond acceptors, hydrogen bond donors and hydrophobic interactions [38]. The data are presented in Table 1.

3.3. HCV NS3/4A genotypes share similar fold but different local interactions

Although the different HCV NS3 genotypes show higher degrees of similarity, there are some variations that make some genotypes less susceptible to treatment and binding of drugs [6,13]. Also, these variations affect the dynamics and enzymatic activities, not just ligand binding. It is reported that the catalytic triad dynamics of 1b, 3a and 4a show different behavior [19–21]. Therefore, the study of sequence and structural relationships of different genotypes to the different designed drugs (in market or in clinical trials) is of utmost importance to reveal the efficacy of drugs to the different genotypes. The present results show that the overall fold and secondary structure are conserved. The binding sites' physicochemical characteristics are not very similar between different genotypes. This indicates the effect of local environment on the geometry and druggability of binding site and, as a consequence, the drug – binding affinity and interactions.

3.4. HCV NS3/4A drugs share some structural features but with different predicted affinities

The drug structures are presented in Fig. 2. They represent different classes, e.g., linear, P1–P3 and P2–P4 macrocycles and bismacrocycle. They share similar peptidomimetic backbone (P1′–P3) with slight differences. P1–P1′ acyl sulfonamide cyclopropyl, P2 proline and P3 tert-

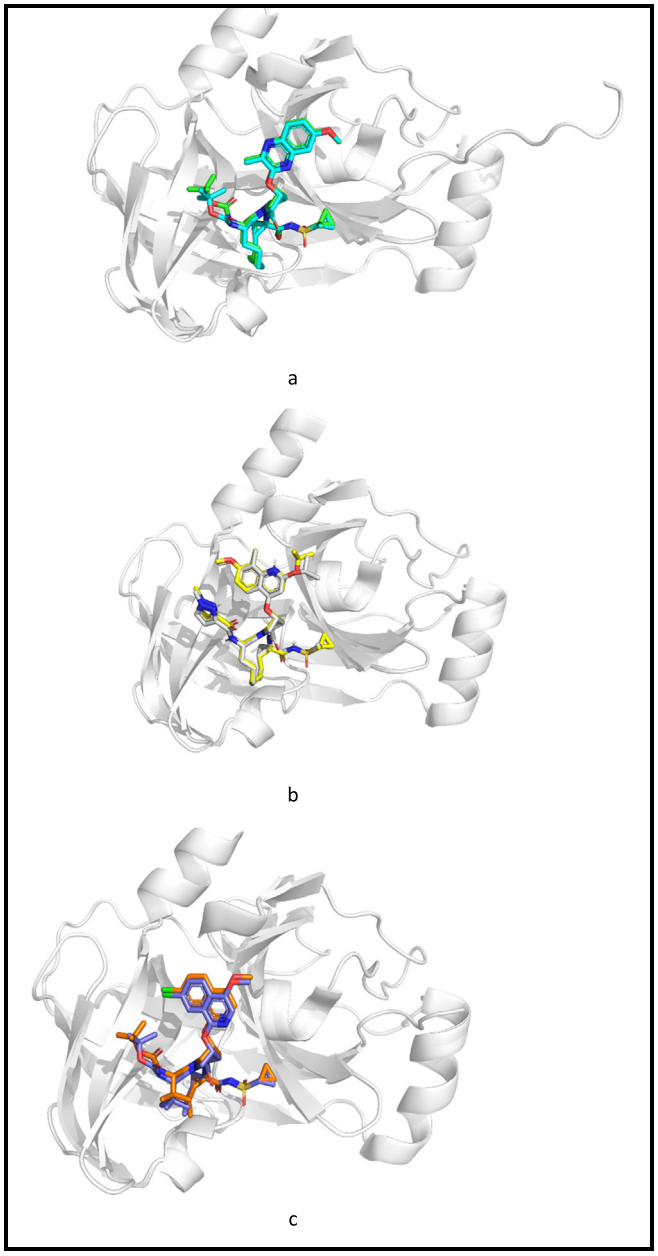

Fig. 3. Presents a superposition between experimental and re-docked structures. [A] 5VOJ (Original Ligand "green", Re-docked Ligand "cyan"). [B] 4I31 (Original Ligand "yellow", Re-docked Ligand "white") [C] 5EQS (Original Ligand "orange", Re-docked Ligand "blue"). (For interpretation of the references to color in this figure legend, the reader is referred to the web version of this article.)

butyl group [5,15]. The only differences are the extended P2 group, P4 capping group and the type of structure, e.g. linear or macrocyclic (P1–P3 or P2–P4) [5,15]. Most of the affinity enhancement comes from the large extended P2 group, but it makes the drug susceptible to resistance because it protrudes from the substrate envelope [47,48]. Second and third generation inhibitors share some structural features, but they vary in binding affinity and genetic barrier to resistance [6,13].

Third generation drugs such as grazoprevir, glecaprevir, paritaprevir and voxilaprevir are pan – genotypic drugs [6,13]. It is reported that they are efficient against different genotypes but with different affinities [6,13]. The present results suggest that no one drug binds tightly to all HCV genotypes based on the predicted binding affinities (docking scores). Some drugs work better with some genotypes while other drugs are efficient against other genotypes. Table 2 shows the mean docking scores of 13 different drugs against 18 genotypes. It also shows whether the differences between docking scores of different drugs are significant or not. Since, the results are based on docking simulation, the docking protocol has been validated. The drugs are re-docked back in their crystal structures as shown in methods section. RMSD values of ligands (experimental and re-docked) are less than 1A˚. The less RMSD value indicates a better reproduction of the binding mode and hence a better docking protocol. Fig. 3 shows a superposition of experimental and re-docked structure. The rmsd value is calculated for the ligand heavy atoms. The rmsd value of 5VOJ is 0.450, while for 4I31 is 0.581. The rmsd value for the third structure 5EQS is 0.445.

The best scoring drug for genotype 1a is simeprevir, then MK6325 and danoprevir, while for 1b, simeprevir and vaniprevir are the best. MK6325 and vaniprevir are the best drugs for treating genotype 1c. Thus, in general, simeprevir and MK6325 are the best drugs for genotype 1. Genotype 2a has lower predicted affinity to drugs. The best drugs for 2a are vaniprevir, paritaprevir, grazoprevir and M6325, while simeprevir and MK2748 are the best for 2b. Genotypes 2b, 2c and 2k have higher predicted affinities compared to 2a. MK2748, paritaprevir and MK6325 are the best drugs for 2c while simeprevir and MK6325 are the best for 2k. So, simeprevir, MK6325, MK2748 and paritaprevir can be considered efficient drugs for genotype 2.

Genotype 3 is one of the most difficult HCV genotypes to treat because it contains several mutations in the binding site that cause resistance [6,13,19]. It contains D168Q and R123T mutations that affect drug binding [13,19]. Grazoprevir, vaniprevir and simeprevir are the best drugs to treat genotype 3a, while paritaprevir and MK2748 are the best for genotype 3b. MK2748 is predicted to be better with genotype 3k. These results suggest that P2–P4 macrocyclic structures like grazoprevir, vaniprevir and MK2748 are the best treatments for genotype 3. MK6325 and paritaprevir are the best drugs for genotype 4a.

Genotype 5a contains several mutations that cause resistance like Q80K and D168E and this reduces drug affinity [13,44,45]. Several drugs have nearly similar predicted affinity to genotype 5a like MK6325, MK2748, vaniprevir and grazoprevir. Also, like genotype 3, the results suggest that P2–P4 macrocyclic structures are the best for genotype 5a. MK2748, vaniprevir and glecaprevir are the best drugs for genotype 6a. This genotype contains Q80K [13,44] mutation that causes resistance and affects structures with larger P2 moiety like simeprevir. The best drug for genotype 6b is simeprevir while MK6325, simeprevir, and vaniprevir are the best ones for genotype 6d. Also, MK6325 and vaniprevir have better affinity to genotypes 6g than the other drugs. Genotype 6h contains the bulkier Y57 instead of the conserved catalytic residue H57. MK2748 and grazoprevir are the best drugs for this genotype. They contain the P2 quinoxaline moiety which stacks against the catalytic residues D81 and H/Y57 [15,47]. The best drugs for genotype 6k are simeprevir and vaniprevir. These results suggest that no one group of drugs can treat genotype 6 variants alone.

Simeprevir is predicted to be one of the best drugs among most genotypes, therefore its binding mode with different genotypes will be discussed in more detail. The protease interactions with other best drugs are presented in tables S2–S8 for danoprevir, glecaprevir, grazoprevir, MK2748, MK6325, paritaprevir and vaniprevir, respectively.

3.5. Binding mode analysis of simeprevir to different genotypes

The interactions of simeprevir with different genotypes are listed in Table 3. Genotypes 1a and 1b have nearly the same binding mode but 1c is different from them especially, the conformation of the large extended P2 moiety. The difference in binding energy between 1a and 1b is probably due to the loss of hydrogen bonding interactions of R155 with the large extended P2 moiety and loss of interactions with the oxyanion hole residues G137 and S138. Genotype 1c has a different

Table 3
The interactions of simeprevir with different genotypes as analyzed using PLIP server.

	Hydrogen bonds	Hydrophobic interactions	Pi – cation interactions
1A	H57,K136,G137,S138,S139,R155,A157	Q41,F43,Y56,H57,D81,I132,K136,F154,A156,A157	
1B	H57,K136,S139,A157	Q41,F43,H57,V132,K136,F154,R155,A156,A157	
1C	Q41,R123,K136,G137,S139,R155	V78,I132,K136,F154,A156	R155
2A	Q41,H57,R123,G137,S139	Q41,Y56,L132,K136,F154,A156	R155
2B	H57,D81,G137,S139,R155	Y56,A78,L132,K136,F154,D168	R155
2C	D81,K136,G137,S139	F43,F56,L132,K136	R155
2K	K136,G137,S138,S139,R155	F43,L132,K136,F154	R155
3A	H57,D81,K136,G137,S138,S139,R155,A157,Q168	F43,Y56,H57,L132,K136,F154,A156,A157	R155
3B	K136,G137,S139,R155	F43,L132,K136	R155
3K	Q41,G137,S139,R155,Q168	Q41,V55,H57,D81,L132,K137,V158	R155
4A	H57,D79,D81,G137,S139,R155	Y56,V78,K136,F154,A156	R155
5A	Q41,K136,S139,R155,E168	K136,R155,A156,E168,V170	
6A	G137,S139,R155	H57,D81,I132,K136,F154,V158	R155
6B	D79,D81,K136,G137,S139,R155	F43,V55,Y56,V78,D81,I132,K136,F154,A157	R155
6D	H57,K136,G137,S138,S139,R155,A157	F43,Y56,V78,L132,K136,F154	R155
6G	Q41,H57,D81,G137,S139,R155,A157	Y56,D81,I132,F154,A157	
6H	D79, K136,G137,S139,R155	Y56,Y57,V78,D81,F154	
6K	H57, K136,G137,S138,S139,R155,A157	Y56,I132,K136,F154,A156,A157	R155

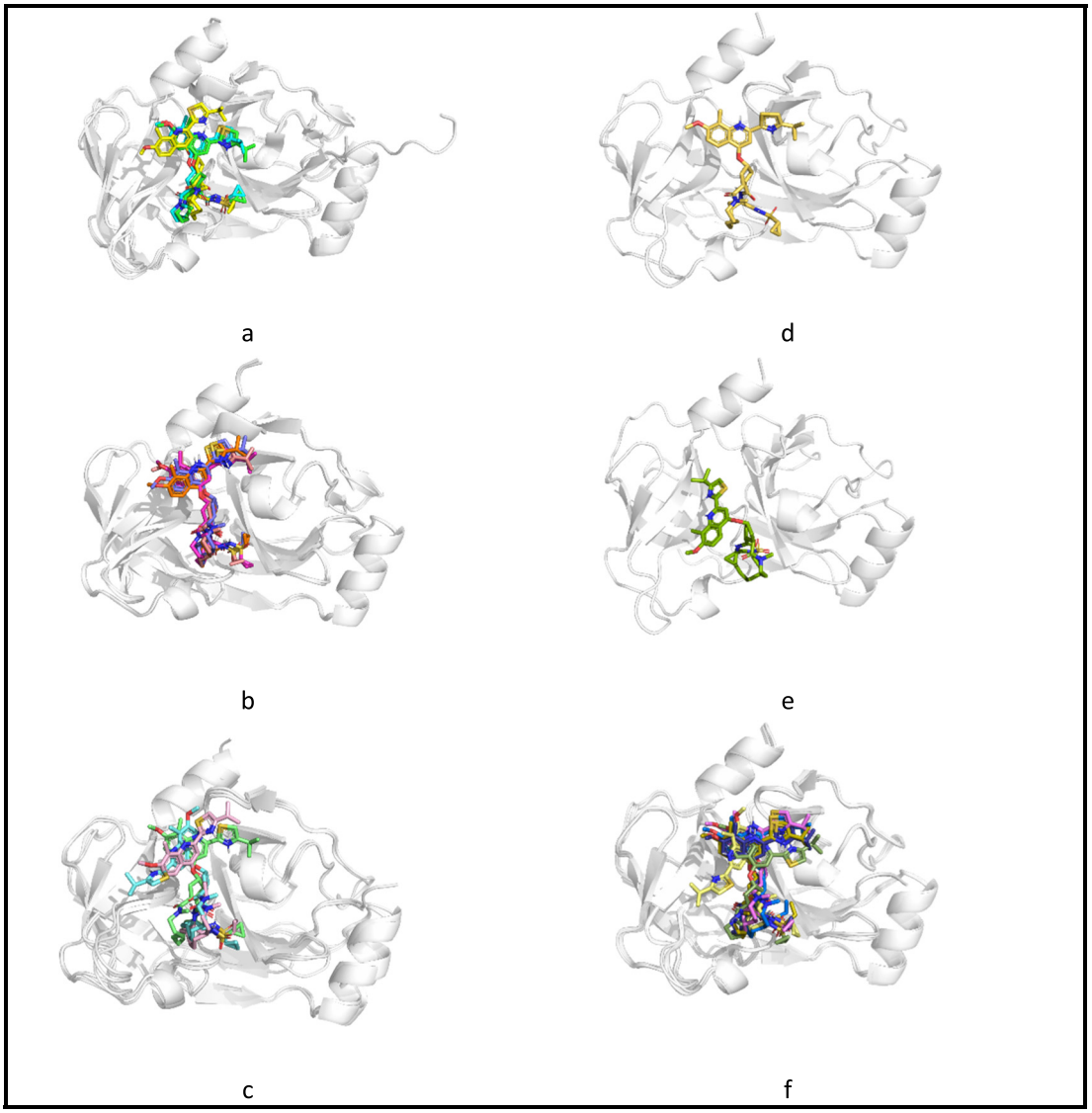

Fig. 4. presents simeprevir binding mode with different genotypes. [A] Simeprevir – genotype 1 (a "green", b "cyan" and c "yellow"). [B] Simeprevir – genotype 2 (a "pink", b "pale pink", c "blue" and k "orange"). [C] Simeprevir – genotype 3 (a "pale green", b "pale pink" and c "pale cyan"). [D] Simeprevir – genotype 4 (a "yellow"). [E] Simeprevir – genotype 5 (a "green"). [F] Simeprevir – genotype 6 (a "pale orange", b "blue", d "orange", g "green", h "pink" and k "deep blue"). (For interpretation of the references to color in this figure legend, the reader is referred to the web version of this article.)

conformation of the large extended P2 moiety, which is oriented far away from the catalytic residues H57 and D81 to interact mainly with R155 through pi – cation interactions. It loses the hydrophobic interactions between H57 and D81 and the hydrogen bond with H57. Also, it loses the conserved hydrogen bond with A157 backbone which is one of the most known recognition interactions of NS3 protease with drugs and substrates [47–52]. The acyl sulfonamide cyclopropyl P1′ moiety is not fitted in S1′ pocket and loses many hydrophobic interactions, especially with Q41 and F43. Hydrophobic interactions are the main driving forces for protease – drug recognition and this is the reason for the decreased binding affinity of 1c with Simeprevir [49–51]. Fig. 4a presents a superposition of genotypes 1a, 1b and 1c complexes with simeprevir.

Genotype 2, subtypes a, b, c and k have predicted binding affinities lower than genotype 1a and 1b. The E1 – F1 loop is not conserved (residues 76–80) and it contains glycine at the position 80 instead of glutamine (Q80G). This position is a drug – resistant site, especially for simeprevir [13,44], where glutamine is mainly mutated to lysine (Q80K), here it is mutated to glycine. Q80 makes hydrogen bond with R155 and allows it to adapt and fit to the large extended P2 moiety of protease inhibitors, especially simeprevir [44,49,50]. When this hydrogen bond is lost due to mutation at this position, R155 becomes more flexible and take different conformations that may not adapt with this large P2 moiety and loses more interactions [44,49,50]. Fig. 4b presents a superposition of genotypes 2a, 2b, 2c and 2k complexes with simeprevir. In genotype 2a, the conformation of the large P2 moiety is different, especially the thiazole ring which makes hydrophobic contacts with H57 in genotype 1a and 1b, but these contacts are lost in 2a. The quinoline ring makes several pi – cation interactions with R155. Also, the acyl sulfonamide cyclopropyl P1′ moiety makes hydrogen bond with Q41 but lose a lot of hydrophobic interactions with S1′ pocket. Genotype 2b, like 2a, has nearly similar extended P2 binding mode, but it has more interactions with catalytic residues and more hydrophobic interactions. Thus, 2b has the best predicted affinity with simeprevir compared with other genotype 2 subtypes. Genotypes 2c and 2k have similar conformation like genotype 1c but the P1′ cyclopropyl moiety is oriented upward. The decreased hydrogen bonding and hydrophobic interactions explain the difference in predicted binding affinity of simeprevir between genotypes 1 and 2.

Genotype 3 is known as the most resistant genotype to the developed drugs because it contains glutamine (Q) at position 168 instead of aspartate and Threonine (T) at position 123 instead of arginine [13,19]. Deletion of charged amino acids (D168 and R123) at these positions disrupts the electrostatic network established with R155 which allows it to adapt to the large P2 moiety of inhibitors and cause decreased binding affinity with the protease [19,45,47,48,50]. Genotype 3a has nearly the same binding conformation as 1a and 1b, but with some deviations of the thiazole ring of the large extended P2 moiety. It shows few hydrophobic interactions compared to genotype 1 and this is reflected in its decreased binding affinity. On contrary, genotypes 3b and 3k have different conformations, especially 3k, where the large extended P2 moiety is inverted. Both of them show decreased hydrogen bonding and hydrophobic interactions compared with genotype 1 and even with genotype 3a. This probably explains the failure of simeprevir as a potential treatment for 3b and 3k. The simeprevir – genotypes 3a, 3b and 3k complexes are presented in Fig. 4c.

The binding mode of simeprevir to genotype 4a differs from that of genotype 1. The acyl sulfonamide cyclopropyl P1′ moiety is not fitted in S1′ pocket and loses interactions with Q41 and F43. So, genotype 4a has a lower predicted binding affinity, and this is most likely due to the decreased hydrophobic interactions with protease compared to genotype 1. Fig. 4d presents a superposition of genotypes 4a complex with simeprevir.

Genotypes 5a and 6a have the lowest predicted binding affinity with simeprevir, especially 5a. Both genotypes contain the drug - resistant mutation Q80K, which, as mentioned before, causes decreased binding of simeprevir. Genotype 5a contains another drug - resistant mutation, D168E which also weakens simeprevir binding [45,50]. Fig. 4e presents a superposition of genotype 5a complex with simeprevir. Genotypes 5a and 6a show the most different binding modes compared with the other genotypes. In genotype 5a, the large P2 group is far away from the catalytic active site residues and it stacks mainly with E168. R155 has a considerably different conformation due to its higher flexibility and it doesn't fit well with the P2 group. These differences may explain the predicted decreased binding affinity of 5a compared to the other genotypes. In genotype 6a, the binding mode of P2 moiety is inverted but it stacks mainly with catalytic residues H57 and D81. It loses a lot of interactions and hence has low predicted binding affinity like 5a.

Genotype 6 subtypes b, d and k have higher predicted affinity to simeprevir compared with the other subtypes a, g and h. They make a lot of hydrogen bonding and hydrophobic interactions and have slightly different binding modes than 1a and 1b. The large extended P2 moiety is shifted upward and loses hydrophobic interactions with catalytic H57. Also, the acyl sulfonamide cyclopropyl P1′ moiety is not fitted in S1′ pocket and loses interactions with Q41. Genotypes 6g and 6h have lower affinities due to loss of many hydrophobic interactions. Genotype 6g has different conformation of the thiazole ring and P1′ cyclopropyl group which affects its interactions. Furthermore, genotype 6h contains the bulkier tyrosine instead of the catalytic histidine at position 57, which makes steric clashes with the large P2 group and affects the binding mode of simeprevir. Fig. 4f presents a superposition of genotypes 6a, 6b, 6d, 6g, 6h and 6k complexes with simeprevir.

Finally, it should be noted that the binding affinities (EC_{50}) of some drugs, such as Glecaprevir [53], Paritaprevir [54], Vaniprevir [55] and Grazoprevir [56], have been measured in replicon cell lines of different genotypes. Unfortunately, the experimental conditions are not the same which make the experimental comparison not feasible. So, this study aims to make computational predication of drug affinities against different genotypes in silico under the same conditions which facilitates the comparison. Future work may consider the design of an experiment to compare drug affinities against different genotypes experimentally under the same conditions.

4. Conclusion

Computational approaches such as homology modeling and molecular docking are widely used in the drug discovery field. The present study predicts 3D structures of different genotypes and their interactions with drugs (in market and in clinical trials). It suggests that no one drug is able to cure all of the different genotypes where more extensive research is still needed to develop such a potent drug. Simeprevir and to a lesser extent MK6325 are the best among the different drugs. They cure many genotypes but they fail against other genotypes as well. P2–P4 macrocyclic drugs, such as grazoprevir, Vaniprevir, glecaprevir and MK2748, show better results against genotypes 2, 3 and 5. This study is expected to help physicians to prescribe the best drug based on the dominant HCV genotype of patient and would further motivate the personalized medicine field.

Appendix A. Supplementary data

Supplementary data to this article can be found online at https://doi.org/10.1016/j.lfs.2018.12.004.

References

[1] A. Petruzziello, S. Marigliano, G. Loquercio, A. Cozzolino, C. Cacciapuoti, Global epidemiology of hepatitis C virus infection: an up-date of the distribution and circulation of hepatitis C virus genotypes, World J. Gastroenterol. 22 (34) (Sep 14 2016) 7824.

[2] A. Zia, S.W. Abbasi, S. Ahmad, M. Zia, A. Raza, Phylogenetic analysis, structure modeling and docking study of HCV NS3 protease for the identification of potent inhibitors, Infect. Genet. Evol. 59 (Apr 30 2018) 51–62.

[3] R. Bartenschlager, V. Lohmann, F. Penin, The molecular and structural basis of advanced antiviral therapy for hepatitis C virus infection, Nat. Rev. Microbiol. 11 (7) (Jul 1 2013) 482–496.
[4] P. Simmonds, J. Bukh, C. Combet, G. Deléage, N. Enomoto, S. Feinstone, P. Halfon, G. Inchauspé, C. Kuiken, G. Maertens, M. Mizokami, Consensus proposals for a unified system of nomenclature of hepatitis C virus genotypes, Hepatology 42 (4) (Oct 1 2005) 962–973.
[5] J.A. McCauley, M.T. Rudd, Hepatitis C virus NS3/4a protease inhibitors, Curr. Opin. Pharmacol. 30 (Oct 1 2016) 84–92.
[6] G. Li, E. De Clercq, Current therapy for chronic hepatitis C: the role of direct-acting antivirals, Antivir. Res. 142 (Jun 1 2017) 83–122.
[7] K.D. Raney, S.D. Sharma, I.M. Moustafa, C.E. Cameron, Hepatitis C virus non-structural protein 3 (HCV NS3): a multifunctional antiviral target, J. Biol. Chem. 235 (30) (May 10 2010) 22725–22731 jbc-R110.
[8] A.A. Ezat, N.S. El-Bialy, H.I. Mostafa, M.A. Ibrahim, Molecular docking investigation of the binding interactions of macrocyclic inhibitors with HCV NS3 protease and its mutants (R155K, D168A and A156V), Protein J. 33 (1) (Feb 1 2014) 32–47.
[9] H.I. Mostafa, N.S. El-Bialy, A.A. Ezat, N.A. Saleh, Ibrahim MA. QSAR analysis and molecular docking simulation of suggested peptidomimetic NS3 protease inhibitors, Curr. Comput. Aided Drug Des. 10 (1) (Mar 2014) 28–40.
[10] K. Li, E. Foy, J.C. Ferreon, M. Nakamura, A.C. Ferreon, M. Ikeda, S.C. Ray, M. Gale, S.M. Lemon, Immune evasion by hepatitis C virus NS3/4A protease-mediated cleavage of the Toll-like receptor 3 adaptor protein TRIF, Proc. Natl. Acad. Sci. 102 (8) (Feb 22 2005) 2992–2997.
[11] R.B. Seth, L. Sun, C.K. Ea, Z.J. Chen, Identification and characterization of MAVS, a mitochondrial antiviral signaling protein that activates NF-κB and IRF3, Cell 122 (5) (Sep 9 2005) 669–682.
[12] K.P. Romano, J.M. Laine, L.M. Deveau, H. Cao, F. Massi, C.A. Schiffer, Molecular mechanisms of viral and host-cell substrate recognition by HCV NS3/4A protease, J. Virol. 85 (13) (Apr 20 2011) 6106–6116 JVI-00377.
[13] M.C. Sorbo, V. Cento, V.C. Di Maio, A.Y. Howe, F. Garcia, C.F. Perno, F. Ceccherini-Silberstein, Hepatitis C virus drug resistance associated substitutions and their clinical relevance: Update 2018, Drug Resist. Updat. 37 (Feb 21 2018) 17–39.
[14] N.K. Yilmaz, R. Swanstrom, C.A. Schiffer, Improving viral protease inhibitors to counter drug resistance, Trends Microbiol. 24 (7) (Jul 1 2016) 547–557.
[15] D.I. Soumana, N. Kurt Yilmaz, K.L. Prachanronarong, C. Aydin, A. Ali, C.A. Schiffer, Structural and thermodynamic effects of macrocyclization in HCV NS3/4A inhibitor MK-5172, ACS Chem. Biol. 11 (4) (Jan 6 2016) 900–909.
[16] L.N. Rusere, A.N. Matthew, G.J. Lockbaum, M. Jahangir, A. Newton, C.J. Petropoulos, W. Huang, N. Kurt Yilmaz, C.A. Schiffer, A. Ali, Quinoxaline-based linear HCV NS3/4A protease inhibitors exhibit potent activity against drug resistant variants, ACS Med. Chem. Lett. 9 (7) (May 17 2018) 691–696.
[17] A.N. Matthew, J. Zephyr, C.J. Hill, M. Jahangir, A. Newton, C.J. Petropoulos, W. Huang, N. Kurt-Yilmaz, C.A. Schiffer, A. Ali, Hepatitis C virus NS3/4A protease inhibitors incorporating flexible P2 quinoxalines target drug resistant viral variants, J. Med. Chem. 60 (13) (Jun 19 2017) 5699–5716.
[18] A.K. Belfrage, E. Abdurakhmanov, E. Åkerblom, P. Brandt, H. Alogheli, J. Neyts, U.H. Danielson, A. Sandström, Pan-NS3 protease inhibitors of hepatitis C virus based on an R3-elongated pyrazinone scaffold, Eur. J. Med. Chem. 148 (Mar 25 2018) 453–464.
[19] D.I. Soumana, N. Kurt Yilmaz, A. Ali, K.L. Prachanronarong, C.A. Schiffer, Molecular and dynamic mechanism underlying drug resistance in genotype 3 hepatitis C NS3/4A protease, J. Am. Chem. Soc. 138 (36) (Sep 2 2016) 11850–11859.
[20] M. Kramer, D. Halleran, M. Rahman, M. Iqbal, M.I. Anwar, S. Sabet, E. Ackad, M. Yousef, Comparative molecular dynamics simulation of hepatitis C virus NS3/4A protease (genotypes 1b, 3a and 4a) predicts conformational instability of the catalytic triad in drug resistant strains, PLoS One 9 (8) (Aug 11 2014) e104425.
[21] H.A. Hamad, J. Thurston, T. Teague, E. Ackad, M.S. Yousef, The NS4A cofactor dependent enhancement of HCV NS3 protease activity correlates with a 4D geometrical measure of the catalytic triad region, PLoS One 11 (12) (Dec 9 2016) e0168002.
[22] M. Mottin, R.C. Braga, R.A. da Silva, J.H. da Silva, A.L. Perryman, S. Ekins, C.H. Andrade, Molecular dynamics simulations of Zika virus NS3 helicase: insights into RNA binding site activity, Biochem. Biophys. Res. Commun. 492 (4) (Oct 28 2017) 643–651.
[23] A. Venkatesan, M. Rambabu, S. Jayanthi, J. Febin Prabhu Dass, Pharmacophore feature prediction and molecular docking approach to identify novel anti-HCV protease inhibitors, J. Cell. Biochem. 119 (1) (Jan 2018) 960–966.
[24] N.A. Saleh, A.A. Ezat, A.A. Elfiky, W.M. Elshemey, M. Ibrahim, Theoretical study on modified boceprevir compounds as NS3 protease inhibitors, J. Comput. Theor. Nanosci. 12 (3) (Mar 1 2015) 371–375.
[25] A.A. Ezat, H.I. Mostafa, N. El-Bialy, N.A. Saleh, M.A. Ibrahim, Computational approaches to study peptidomimetic and macrocyclic hepatitis C virus NS3 protease inhibitors, J. Comput. Theor. Nanosci. 12 (1) (Jan 1 2015) 52–59.
[26] N.A. Saleh, A.A. Elfiky, A.A. Ezat, W.M. Elshemey, M. Ibrahim, The electronic and quantitative structure activity relationship properties of modified telaprevir compounds as HCV NS3 protease inhibitors, J. Comput. Theor. Nanosci. 11 (2) (Feb 1 2014) 544–548.
[27] C. Zhang, T. Feng, J. Cheng, Y. Li, X. Yin, W. Zeng, X. Jin, Y. Li, F. Guo, T. Jin, Structure of the NS5 methyltransferase from Zika virus and implications in inhibitor design, Biochem. Biophys. Res. Commun. 492 (4) (Oct 28 2017) 624–630.
[28] P. Polamreddy, V. Vishwakarma, P. Saxena, Identification of potential anti-hepatitis C virus agents targeting non structural protein 5B using computational techniques, J. Cell. Biochem. 119 (10) (Jul 30 2018) 8574–8587.
[29] C. Nithin, P. Ghosh, J. Bujnicki, Bioinformatics tools and benchmarks for computational docking and 3D structure prediction of RNA-protein complexes, Genes 9 (9) (Aug 25 2018) 432.
[30] UniProt Consortium, UniProt: the universal protein knowledgebase, Nucleic Acids Res. 46 (5) (Mar 16 2018) 2699.
[31] R.C. Edgar, MUSCLE: multiple sequence alignment with high accuracy and high throughput, Nucleic Acids Res. 32 (5) (Mar 1 2004) 1792–1797.
[32] X. Robert, P. Gouet, Deciphering key features in protein structures with the new ENDscript server, Nucleic Acids Res. 42 (W1) (Apr 21 2014) W320–W324.
[33] J.A. O'Meara, C.T. Lemke, C. Godbout, G. Kukolj, L. Lagacé, B. Moreau, D. Thibeault, P.W. White, M. Llinàs-Brunet, Molecular mechanism by which a potent hepatitis C virus NS3-NS4A protease inhibitor overcomes emergence of resistance, J. Biol. Chem. 288 (8) (Feb 22 2013) 5673–5681.
[34] L. Bordoli, F. Kiefer, K. Arnold, P. Benkert, J. Battey, T. Schwede, Protein structure homology modeling using SWISS-MODEL workspace, Nat. Protoc. 4 (1) (Dec 2008) 1.
[35] L. Heo, H. Park, C. Seok, GalaxyRefine: protein structure refinement driven by side-chain repacking, Nucleic Acids Res. 41 (W1) (May 21 2013) W384–W388.
[36] http://servicesn.mbi.ucla.edu/SAVES/.
[37] I.W. Davis, A. Leaver-Fay, V.B. Chen, J.N. Block, G.J. Kapral, X. Wang, L.W. Murray, I.I.I.W.B. Arendall, J. Snoeyink, J.S. Richardson, D.C. Richardson, MolProbity: all-atom contacts and structure validation for proteins and nucleic acids, Nucleic Acids Res. 35 (Suppl. 2) (Jul 1 2007) W375–W383.
[38] R. Fährrolfes, S. Bietz, F. Flachsenberg, A. Meyder, E. Nittinger, T. Otto, A. Volkamer, M. Rarey, Proteins Plus: a web portal for structure analysis of macromolecules, Nucleic Acids Res. 45 (W1) (May 2 2017) W337–W343.
[39] N.M. O'Boyle, M. Banck, C.A. James, C. Morley, T. Vandermeersch, G.R. Hutchison, Open Babel: An open chemical toolbox, J. Cheminf. 3 (1) (Dec 2011) 33.
[40] A. Gaulton, A. Hersey, M. Nowotka, A.P. Bento, J. Chambers, D. Mendez, P. Mutowo, F. Atkinson, L.J. Bellis, E. Cibrián-Uhalte, M. Davies, The ChEMBL database in 2017, Nucleic Acids Res. 45 (D1) (Nov 28 2016) D945–D954.
[41] O. Trott, A.J. Olson, AutoDock Vina: improving the speed and accuracy of docking with a new scoring function, efficient optimization, and multithreading, J. Comput. Chem. 31 (2) (Jan 30 2010) 455–461.
[42] S. Forli, R. Huey, M.E. Pique, M.F. Sanner, D.S. Goodsell, A.J. Olson, Computational protein–ligand docking and virtual drug screening with the AutoDock suite, Nat. Protoc. 11 (5) (2016 May) 905.
[43] S. Salentin, S. Schreiber, V.J. Haupt, M.F. Adasme, M. Schroeder, PLIP: fully automated protein–ligand interaction profiler, Nucleic Acids Res. 43 (W1) (Apr 14 2015) W443–W447.
[44] Z. Guo, S. Black, Y. Hu, P. McMonagle, P. Ingravallo, R. Chase, S. Curry, E. Asante-Appiah, Unraveling the structural basis of grazoprevir potency against clinically relevant substitutions in hepatitis C virus NS3/4A protease from genotype 1a, J. Biol. Chem. 292 (15) (Feb 21 2017) 6202–6212 jbc-M116.
[45] D. Pan, W. Xue, W. Zhang, H. Liu, X. Yao, Understanding the drug resistance mechanism of hepatitis C virus NS3/4A to ITMN-191 due to R155K, A156V, D168A/E mutations: A computational study, Biochim. Biophys. Acta Gen. Subj. 1820 (10) (Oct 1 2012) 1526–1534.
[46] M. Feig, Computational protein structure refinement: almost there, yet still so far to go, Wiley Interdiscip. Rev.: Comput. Mol. Sci. 7 (3) (May 2017) e1307.
[47] K.P. Romano, A. Ali, C. Aydin, D. Soumana, A. Özen, L.M. Deveau, C. Silver, H. Cao, A. Newton, C.J. Petropoulos, W. Huang, The molecular basis of drug resistance against hepatitis C virus NS3/4A protease inhibitors, PLoS Pathog. 8 (7) (Jul 26 2012) e1002832.
[48] K.P. Romano, A. Ali, W.E. Royer, C.A. Schiffer, Drug resistance against HCV NS3/4A inhibitors is defined by the balance of substrate recognition versus inhibitor binding, Proc. Natl. Acad. Sci. 107 (49) (Dec 7 2010) 20986–20991.
[49] M.D. Cummings, J. Lindberg, T.I. Lin, H. de Kock, O. Lenz, E. Lilja, S. Felländer, V. Baraznenok, S. Nyström, M. Nilsson, L. Vrang, Induced-fit binding of the macrocyclic noncovalent inhibitor TMC435 to its HCV NS3/NS4A protease target, Angew. Chem. 122 (9) (Feb 22 2010) 1696–1699.
[50] W. Xue, D. Pan, Y. Yang, H. Liu, X. Yao, Molecular modeling study on the resistance mechanism of HCV NS3/4A serine protease mutants R155K, A156V and D168A to TMC435, Antivir. Res. 93 (1) (Jan 1 2012) 126–137.
[51] Y. Guan, H. Sun, Y. Li, P. Pan, D. Li, T. Hou, The competitive binding between inhibitors and substrates of HCV NS3/4A protease: a general mechanism of drug resistance, Antivir. Res. 103 (Mar 1 2014) 60–70.
[52] A. Meeprasert, S. Hannongbua, T. Rungrotmongkol, Key binding and susceptibility of NS3/4A serine protease inhibitors against hepatitis C virus, J. Chem. Inf. Model. 54 (4) (Apr 1 2014) 1208–1217.
[53] E.J. Lawitz, W.D. O'Riordan, A. Asatryan, B.L. Freilich, T.D. Box, J.S. Overcash, S. Lovell, T.I. Ng, W. Liu, A. Campbell, C.W. Lin, Potent antiviral activities of the direct-acting antivirals ABT-493 and ABT-530 with three-day monotherapy for hepatitis C virus genotype 1 infection, Antimicrob. Agents Chemother. 60 (3) (Mar 1 2016) 1546–1555.
[54] T. Pilot-Matias, R. Tripathi, D. Cohen, I. Gaultier, T. Dekhtyar, L. Lu, T. Reisch, M. Irvin, T. Hopkins, R. Pithawalla, T. Middleton, In vitro and in vivo antiviral activity and resistance profile of the hepatitis C virus NS3/4A protease inhibitor ABT-450, Antimicrob. Agents Chemother. 59 (2) (Feb 1 2015) 988–997.
[55] N.J. Liverton, S.S. Carroll, J. Dimuzio, C. Fandozzi, D.J. Graham, D. Hazuda, M.K. Holloway, S.W. Ludmerer, J.A. McCauley, C.J. McIntyre, D.B. Olsen, MK-7009, a potent and selective inhibitor of hepatitis C virus NS3/4A protease, Antimicrob. Agents Chemother. 54 (1) (Jan 1 2010) 305–311.
[56] F.C. Lahser, K. Bystol, S. Curry, P. McMonagle, E. Xia, P. Ingravallo, R. Chase, R. Liu, T. Black, D. Hazuda, A.Y. Howe, The combination of grazoprevir, a HCV NS3/4A protease inhibitor, and elbasvir, a HCV NS5A inhibitor, demonstrates a high genetic barrier to resistance in HCV genotype 1a replicons, Antimicrob. Agents Chemother. 60 (Feb 29 2016) 2954–2964. AAC-00051.